

Normal Spectral Emissivity Models of Steel 304 at 800–1100 K with an Oxide Layer on the Specimen Surface

Wenjie Zhu¹ · Deheng Shi¹ · Zunlue Zhu¹ · Jinfeng Sun¹

Received: 31 December 2015 / Accepted: 13 May 2016 / Published online: 16 June 2016
© The Indian Institute of Metals - IIM 2016

Abstract This work investigated the normal spectral emissivity characteristics of Steel 304 over a temperature range from 800 to 1100 K and a wavelength range from 1.4 to 2.1 μm . In the experiments, specimens were heated in air for 6 h at a certain temperature. Two platinum–rhodium thermocouples were symmetrically welded onto the front surface of the specimens near the measuring area for accurate monitoring of the surface temperature. The temperatures measured by the two thermocouples had an uncertainty of 1 K. The average of their readings was regarded as the temperature of the specimen surface. The radiance stemming from the specimens were measured at temperatures from 800 to 1100 K in increments of 20 K by multispectral radiation thermometry. Variation in the normal spectral emissivity with respect to wavelength and temperature was studied for different heating times. The effect of surface oxidization on the accurate prediction of the specimen surface temperature was discussed. Similar variation in the normal spectral emissivity for different heating times showed that the emissivity followed a certain rule. Nine emissivity models were examined for accuracy in the temperature prediction. The results showed that the four-parameter log-linear wavelength and line wavelength emissivity models generated best overall temperature prediction. We concluded that the effect of surface oxidization on the emissivity models of Steel 304 could be dismissed; and that the same models could be used to predict its surface temperature from 800 to 1100 K.

Keywords Oxide layer · Steel 304 · Temperature measurement · Multispectral radiation thermometry · Normal spectral emissivity model

1 Introduction

Radiation thermometry subject may be sub-divided into single-wavelength thermometry and multispectral radiation thermometry. To determine the temperature accurately using single-wavelength thermometry, we must know the accurate spectral emissivity of an object. In multispectral radiation thermometry, we must have prior knowledge of the spectral emissivity, wavelength, and temperature [1]. However, spectral emissivity sometimes depends drastically on the wavelength and temperature, and it may be sensitive to emission angle, surface roughness, surface oxidization state, presence of pollutants, and composition of the object [2–4]. As it is difficult to accurately measure the spectral emissivity of a target, it becomes even more difficult to accurately measure the variation in the spectral emissivity with respect to wavelength and temperature under various surface conditions. In particular, gaining knowledge about the spectral emissivity, wavelength, and temperature possibly becomes more complicated when the surface of a target is oxidized in air for a long time.

Experiments [2, 3, 5–14] have been conducted to study the spectral emissivity variation due to the growth of an oxide layer on the steel surface. For example, in 1999, Kobayashi et al. [5] measured the time variation in the spectral emissivity of several kinds of steels over a wavelength range of 0.55 to 5.3 μm and temperature range of 1053 to 1473 K. In 2000, Furukawa and Iuchi [2] studied the variation in the spectral emissivity of cold-rolled steel materials with respect to heating time at wavelengths of

✉ Deheng Shi
scattering@sina.com.cn

¹ College of Physics and Electronic Engineering, Henan Normal University, Xinxiang 453007, China

1.35, 1.55, and 2.2 μm at 873 K. In 2006, Campo et al. [3] measured the directional spectral emissivity of Armco iron at 1.28–25 μm from ambient temperature to 1050 K. Moreover, in 2007, Pujana et al. [7] evaluated the variation in the spectral emissivity of Steel 42CrMo₄ with respect to heating time at wavelengths of 2.12, 4.0, and 8.0 μm and temperatures of 959 and 1073 K. Nevertheless, these investigations [2, 3, 5, 7] evaluated only the effect of heating time on the spectral emissivity of various steels; they did not evaluate the variation in spectral emissivity with respect to the wavelength and temperature.

Additional studies have been recently conducted. In 2010, Wen and Lu [8] studied the variation in spectral emissivity for six types of steels with respect to wavelength and temperature over a range of 2.91 to 4.13 μm at 700, 800, and 900 K. Furthermore, in 2010, Wen [9] measured the effect of heating time on the spectral emissivity of six types of steel materials and evaluated the spectral emissivity variation with respect to wavelength and temperature over a wavelength range from 1.2 to 4.8 μm at 700, 800, and 900 K. Using these same temperature, Wen [10], in 2011, measured the spectral emissivity of several types of steels, and discussed the spectral emissivity variation with respect to wavelength (from 2.0 to 4.8 μm) and temperature. Although these investigations [8–10] studied the effect of heating time on spectral emissivity and evaluated spectral emissivity variation with respect to wavelength and temperature, they did not discuss the effect of heating time on spectral emissivity models. Very recently, our group [6, 11–14] quantitatively studied the effect of heating time on normal spectral emissivity over a temperature range of 800–1100 K at 1.5 μm for several types of steel materials. At that time, we did not evaluate the relationship between the spectral emissivity, wavelength, and temperature.

As reported in our earlier papers [6, 11–14], oxidation on a steel surface can significantly affect normal spectral emissivity and bring about obvious temperature measurement uncertainty. As we know, the accuracy of temperature measurement is greatly dependent on the spectral emissivity model employed in multispectral radiation thermometry. Does surface oxidation affect the normal spectral emissivity model? This question has not been answered clearly by any previous work, which is therefore the motivation for this work.

In this study, we have selected Steel 304 as the target, because no spectral emissivity model has been reported for this type of steel, let alone the effect of heating time on the spectral emissivity model. In the present study, only the normal spectral emissivity has been investigated. In the next section, the measurement principle and experimental procedure of the experimental setup have been briefly

described. In Sect. 3, the normal spectral emissivity measurement of the Steel 304 specimens has been reported for 1.4–2.1 μm at 800 to 1100 K. Nine emissivity models have been examined for accuracy in temperature prediction at various surface oxidation conditions.

2 Materials and Methods

2.1 Experimental Principle

In our experiments, multispectral radiation thermometry was employed to measure the radiation stemming from the surface of the specimens. The thermometry involved eight wavelengths: 1.4, 1.5, 1.6, 1.7, 1.8, 1.9, 2.0, and 2.1 μm . The bandwidth of each wavelength was approximately 20 nm. An eddy current heater was used to heat the specimens to a certain temperature. Two thermocouples were symmetrically welded onto the front surface of the specimens near the measuring area viewed by the InGaAs photodiode detector used in thermometry. The thermocouples were then used to measure the surface temperature of the specimens. It should be noted that the detector must be perpendicular to the surface of the specimens to measure the normal spectral emissivity as accurately as possible.

Assuming that the i th wavelength of thermometry is λ_i ($i = 1, 2, 3, 4, 5, 6, 7,$ and 8 for 1.4, 1.5, 1.6, 1.7, 1.8, 1.9, 2.0, and 2.1 μm , respectively), we used the following equation [6] to determine the normal radiance P_i of the real surface as received by the detector

$$P_i = \frac{\pi^2}{4} \left(\frac{D}{f'} \right)^2 A \int_{\lambda_{i1}}^{\lambda_{i2}} \tau_\lambda \varepsilon(\lambda, T) L_{\lambda, T} d\lambda, \quad (1)$$

where T is the temperature of the specimen surface, P_i is the radiance stemming from the specimen surface at λ_i and D and f' are the aperture diameter and focal length, respectively, of optical receiving system in thermometry, A is the area of the sensitive unit of the detector, λ_{i1} and λ_{i2} are the spectral limits of the optical receiving system used to select the spectral band of the i th wavelength, τ_λ is the total transmissivity of the atmosphere and optical receiving system, and $\varepsilon(\lambda, T)$ is the normal spectral emissivity of the specimen surface at λ and T . With the help of Planck's law, we can re-write Eq. (1) as

$$P_i = \frac{\pi^2}{4} \left(\frac{D}{f'} \right)^2 A \int_{\lambda_{i1}}^{\lambda_{i2}} \tau_\lambda \varepsilon(\lambda, T) 2\pi hc^2 \lambda^{-5} \left[\exp\left(\frac{hc}{\lambda kT}\right) - 1 \right]^{-1} d\lambda, \quad (2)$$

where h is the Planck's constant, c is the speed of light, and k is the Boltzmann constant. The band-width ($\Delta\lambda$) of each interference filter was very narrow (approximately 20 nm). Within such a narrow bandwidth, we could approximately

regard τ_λ and $\varepsilon(\lambda, T)$ as constants at a certain temperature, although τ_λ and $\varepsilon(\lambda, T)$ were never constant between λ_{i1} and λ_{i2} . With these considerations, Eq. (2) may be simplified to

$$P_i = C_i \cdot \varepsilon(\lambda_i, T) \left[\exp\left(\frac{hc}{\lambda_i kT}\right) - 1 \right]^{-1}, \tag{3}$$

by considering

$$C_i = \frac{\pi^3}{2} \left(\frac{D}{f'}\right)^2 A \tau_{\lambda_i} hc^2 \lambda_i^{-5} \Delta\lambda. \tag{4}$$

In Eq. (4), D , f' , A , τ_{λ_i} , λ_i and $\Delta\lambda$ are the parameters of thermometry. These parameters were constant for the i th wavelength. Obviously, C_i was the same for all the specimens used in the experiment. C_i could be accurately evaluated as one of the instrument parameters for each wavelength only if the configuration of the experimental setup did not change. It should be noted that $\varepsilon_{\lambda_i} = \varepsilon(\lambda, T)$ in Eq. (3) was the spectral emissivity model used to infer the surface temperature in thermometry.

We used Eq. (3) combined with the least-squares technique to infer the temperature. For the i th wavelength, assuming that the measured radiance stemming from the specimen surface was $P_{meas,i}$ and that the radiance calculated according to Eq. (3) was $P_{cal,i}$, we could determine the temperature (T) by minimizing the magnitude using the following expression

$$\chi^2 = \sum_{i=1}^8 (P_{meas,i} - P_{cal,i})^2. \tag{5}$$

To determine $P_{cal,i}$ according to Eq. (3), a knowledge of the analytical expression $\varepsilon(\lambda, T)$ was required. Finding the most suitable expression for $\varepsilon(\lambda, T)$ in thermometry was the aim of this study.

2.2 Experimental Setup

The experimental setup consisted of two modules. One was the specimen-heating and temperature-controlling system, which was mainly composed of two R-type platinum–rhodium thermocouples, one temperature-controlling assembly, one eddy current heater, one specimen. The other module was the thermometry, which mainly consisted of one InGaAs photodiode detector, eight pieces of interference filters, one chopper wheel, and one signal-controlling and data-computing system.

The working process of this experimental setup has briefly been outlined below. The eddy current heater was employed to heat the specimen to a certain temperature. As mentioned above, the InGaAs photodiode detector was perpendicular to the specimen surface. The chopper wheel rotated at a speed of 13 r/min, and contained eight equally-spaced pieces of narrow-band interference filters. When the

chopper wheel covered one revolution, the InGaAs photodiode detector received the radiant energy, P_i ($i = 1, 2, 3, 4, 5, 6, 7,$ and 8), that came from the specimen. The radiance received by the detector was converted into a voltage signal for further processing. We then evaluated the temperature (T) of the specimen surface using Eq. (5) for a given emissivity model. In the experiments, each specimen was rectangular in shape with dimensions of approximately 10 cm × 7 cm, and its surface was specular and bright. The distance from the detector to the specimen surface was approximately 0.5 m, and the detector sensed a circular area which was approximately 5 mm in diameter on the specimen surface. The surrounding temperature of the InGaAs detector was well stabilized by the cooling water system.

In the experiments, the temperature (T_0) of the specimen surface was determined by averaging the readings of the two thermocouples. T_0 was regarded as the real temperature of the specimen surface. By comparing T_0 with T (obtained by thermometry), we evaluated the suitability of the emissivity model used to infer the temperature. We examined nine emissivity models for accuracy in the temperature prediction.

One important thing was to maintain the specimen at a certain temperature during the whole experimental period. In our experiments, we accomplished this by using the temperature-controlling assembly. The assembly was mainly composed of a microcomputer-controlled proportional-integral-derivative device, which used the two thermocouples symmetrically welded onto the front surface of the specimen near the measuring area viewed by the detector. If the temperatures measured by the two thermocouples were close to the given value within the 1 K uncertainty, we considered the temperature distribution on the specimen surface homogeneous and invariable.

3 Results and Discussion

We used this experimental setup to investigate the normal spectral emissivity characteristics of Steel 304 specimens over a wavelength range of 1.4 to 2.1 μm. The measurements were done with temperatures varying from 800 to 1100 K in increments of 20 K. Previous experimental results [11] showed that it took approximately 6 h to achieve fully-saturated oxidization on the surface of Steel 304, the specimens in the current study were heated in air for only 6 h at a certain temperature. Because the chopper wheel in the thermometry rotated at a constant speed of 13 r/min, we could get 13 radiant values in 1 min for a certain wavelength. To eliminate random errors in the experiment, we took the average of these 13 experimental values measured within 1 min as the final radiance at that wavelength for a certain heating time. For example, during the tenth minute (from 10 min 0 s to 10 min

59 s), we measured 13 radiance values for each wavelength, and their average was regarded as the radiance for the specific heating time i.e. the tenth minute, at that wavelength.

To accurately evaluate the relationships between the normal spectral emissivity of the specimens and the wavelength and temperature, we measured the normal spectral emissivity at eight wavelengths in thermometry at a certain temperature. To realize such measurements of normal spectral emissivity in the experiment, we regarded each wavelength as a single-wavelength setup, as described in our earlier paper [11–14]. Similar to the radiances discussed above, we also took the average of these 13 normal spectral emissivity results obtained in one minute and regarded it as the normal spectral emissivity at that wavelength for a certain heating time. Employing these experimental results, we could directly determine the relationship between the normal spectral emissivity and wavelength. Such a relationship could be used in thermometry. For clarity in this paper, Fig. 1 shows only the variation in the normal spectral emissivity with respect to wavelength for results obtained at 820, 900, 1000, and 1100 K. For each temperature, we only depicted the variation in the normal spectral emissivity with respect to

wavelength for the heating times of 30, 120, 210, and 300 min, respectively.

At each temperature, we used three pieces of specimens to perform the measurements. For each specimen, we measured the normal spectral emissivity and radiance for each wavelength at a certain temperature. By comparing the variation in the normal spectral emissivity with respect to heating time at a certain wavelength and a certain temperature, we found that the reproducibility of the normal spectral emissivity of Steel 304 was excellent. This excellent reproducibility indicated that random errors in the experiment did not generate any observable effect on the experimental results. In particular, at 1.5 μm , the present normal spectral emissivity results closely reproduced the earlier measurements [11] regarding the variation in the normal spectral emissivity with respect to heating time.

To avoid repetition from our earlier paper [11], here we briefly summarized only the variation of each spectral emissivity curve for a certain heating time. At a certain temperature and wavelength, only one strong oscillation of normal spectral emissivity occurred over the heating duration. All the strong oscillations appeared within 20 min from the start of heating. Similar to our earlier

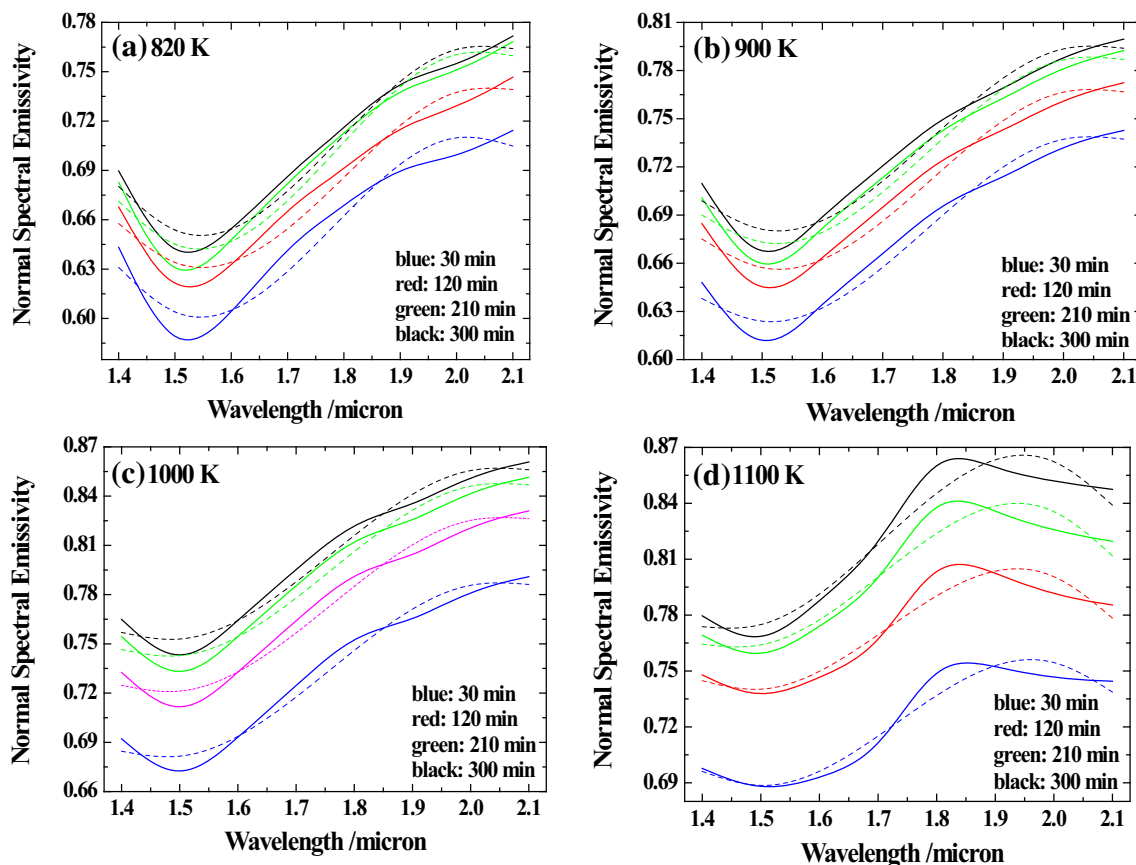


Fig. 1 Curves of normal spectral emissivity of Steel 304 versus wavelength at a certain heating time. Solid line: experimental results, dashed line: results fitted by the four-parameter LWE model

results [11], the strong oscillations originated from the interference effect between the radiation coming from the oxide layer on the specimen surface and the radiation stemming from the substrate. Moreover, the normal spectral emissivity rapidly increased approximately within the initial 200 min of heating time. Thereafter, the surface oxidization slowed down as the heating time increased. Accordingly, the spectral emissivity curves for heating times became flatter.

From Fig. 1, we noticed two important features about the variation in the normal spectral emissivity with respect to wavelength. One was that, the normal spectral emissivity increased on the whole with the increase in wavelength. This suggested that the emissivity models used for Steel 304 should possess such a feature. The other important feature was that all the normal spectral emissivity curves closely followed the same trend for different heating times, which suggested that we could employ an emissivity model that produced these curves.

From Fig. 1d, a decrease in the normal spectral emissivity for 1100 K after 1.8 μm was observed. We did not understand the intrinsic nature of such a decrease; however, by carefully comparing the spectral emissivity curves between different specimens at 1100 K, we found that their reproducibility was excellent. Owing to the excellent reproducibility, we concluded that the decrease in the spectral emissivity for 1100 K after 1.8 μm did not occur due to random errors.

We used the least-squares technique, described in Sect. 2, to infer the surface temperature of the specimens. Table 1 shows the nine emissivity models examined for accuracy in the prediction of temperatures. These emissivity models had been used by Wen and Mudawar [15] in the temperature prediction of roughed aluminum alloys. All the models collected in Table 1 had the feature that the normal spectral emissivity increased in general with the increase in wavelength. Taking into considerations the categories made by Wen and Mudawar [15], we divided the nine emissivity models into four groups: the log-linear wavelength (LLW) emissivity model, the linear wavelength (LWE) emissivity model, the log-linear root-

wavelength (LLRW) emissivity model, and the log-linear wavelength temperature (LLWT) emissivity model.

3.1 Emissivity Models Obtained Directly by Fitting the Normal Spectral Emissivity

Using the normal spectral emissivity obtained by experiment and the mathematical functions collected in Table 1, we evaluated the relationships between the normal spectral emissivity and the wavelength and temperature. Overall, we found that the LLW and LWE models gave the best results. For the LLW and LWE models, the fitting results improved as the number of fitting parameters increased. In other words, the four-parameter LLW and LWE models gave the best overall fitting curves. Tables 2, 3, 4 and 5 show the fitting parameters ($a_1, a_2, a_3,$ and a_4) in combination with the root-mean-square error (E_{RMSE}) and the correlation coefficient (R) obtained in the fitting process at 820, 900, 1000, and 1100 K, respectively. In Table 2, T_0 is the surface temperature of specimens measured by the thermocouples, and t represents the heating time in min from the start of heating. To avoid congestion, Fig. 1 depicts only the fitting curves obtained by the four-parameter LWE model.

Table 2 displays the fitting parameters of the four-parameter LLW and LWE models at 820 K. By comparing the E_{RMSE} and R values between the LLW and LWE models, we found that both models gave excellent fitting results. To some extent, the fitting quality of the LWE model seemed to be slightly superior to that of the LLW model. More importantly, from Table 2, we found that the E_{RMSE} and R values at different heating times were almost same. We also clearly observed from Fig. 1 that the fitting quality essentially did not change with heating times. This suggested that the effect of surface oxidization on the emissivity models of Steel 304 could be ignored at 820 K.

Tables 3 and 4 present the fitting results obtained at 900 and 1000 K, respectively, for heating times of 30, 120, 210, and 300 min. By comparing E_{RMSE} and R , we derived the same conclusions as those at 820 K. The conclusions are as follows: (1) The fitting quality essentially did not vary over

Table 1 Mathematical models of the normal spectral emissivity examined in this work

Model	Mathematical function	Model	Mathematical function
LLW	$\epsilon_\lambda = \exp(a_0 + a_1\lambda)$	LWE	$\epsilon_\lambda = a_0 + a_1\lambda$
	$\epsilon_\lambda = \exp(a_0 + a_1\lambda + a_2\lambda^2)$		$\epsilon_\lambda = a_0 + a_1\lambda + a_2\lambda^2$
	$\epsilon_\lambda = \exp(a_0 + a_1\lambda + a_2\lambda^2 + a_3\lambda^3)$		$\epsilon_\lambda = a_0 + a_1\lambda + a_2\lambda^2 + a_3\lambda^3$
LLRW	$\epsilon_\lambda = \exp(a_0\sqrt{\lambda})$	LLWT	$\epsilon_\lambda = \exp(a_0\lambda + a_1T)$
	$\epsilon_\lambda = \exp(a_0 + a_1\sqrt{\lambda})$		

Table 2 Fitting results of the four-parameter LLW and LWE models at 820 K and 30, 120, 210, and 300 min from the start of heating

T_0/K	t/min	a_0	a_1	a_2	a_3	E_{RMSE}	R
LWE	30	11.9087	-19.7021	11.2742	-2.1109	0.0139	0.9527
	120	10.6791	-17.4244	9.9130	-1.8427	0.0109	0.9700
	210	11.8398	-19.4874	11.1295	-2.0773	0.0129	0.9658
	300	11.4627	-18.7753	10.6998	-1.9929	0.0108	0.9735
LLW	30	16.5729	-29.7544	17.0239	-3.1869	0.0146	0.9478
	120	14.2705	-25.5459	14.5369	-2.7032	0.0115	0.9668
	210	15.4715	-27.6957	15.8201	-2.9535	0.0135	0.9620
	300	14.8934	-26.6101	15.1683	-2.8262	0.0114	0.9703

Table 3 Fitting results of the four-parameter LLW and LWE models at 900 K and 30, 120, 210, and 300 min from the start of heating

T_0/K	t/min	a_0	a_1	a_2	a_3	E_{RMSE}	R
LWE	30	9.3778	-15.4072	8.8833	-1.6694	0.0111	0.9727
	120	9.9428	-16.2535	9.3256	-1.7460	0.0106	0.9734
	210	10.0767	-16.4904	9.4772	-1.7768	0.0117	0.9704
	300	10.1192	-16.5281	9.4866	-1.7765	0.0118	0.9695
LLW	30	12.1879	-22.3019	12.8711	-2.4209	0.0116	0.9700
	120	12.5477	-22.7082	13.0363	-2.4421	0.0111	0.9706
	210	12.3800	-22.4153	12.8904	-2.4181	0.0122	0.9676
	300	12.3306	-22.2758	12.7927	-2.3969	0.0122	0.9667

Table 4 Fitting results of the four-parameter LLW and LWE models at 1000 K and 30, 120, 210, and 300 min from the start of heating

T_0/K	t/min	a_0	a_1	a_2	a_3	E_{RMSE}	R
LWE	30	7.0630	-11.3985	6.6534	-1.2614	0.0087	0.9801
	120	7.1086	-11.3932	6.6411	-1.2573	0.0091	0.9788
	210	7.1604	-11.4440	6.6699	-1.2629	0.0089	0.9789
	300	7.2293	-11.5444	6.7270	-1.2737	0.0090	0.9783
LLW	30	8.0134	-15.0354	8.7959	-1.6704	0.0092	0.9782
	120	7.6755	-14.3053	8.3554	-1.5843	0.0095	0.9769
	210	7.5434	-14.0106	8.1812	-1.5513	0.0094	0.9770
	300	7.5377	-13.9694	8.1546	-1.5462	0.0094	0.9765

different heating times; (2) both the LWE and LLW models gave excellent fitting results; and (3) the fitting quality of the LWE model was slightly superior to that of the LLW model. We also concluded that the effect of surface oxidation on the emissivity models of Steel 304 could be ignored at 900 and 1000 K.

Table 5 presents the fitting results obtained at 1100 K for the heating times of 30, 120, 210, and 300 min. From Table 5, we were able to conclude that the effect of surface oxidation on the emissivity models of Steel 304 could be dismissed at 1100 K as well. As depicted in Fig. 1, the

decrease in the experimental spectral emissivity after 1.8 μm was well reproduced by the fitting curves.

Summarizing the above discussion, we reached at three main conclusions. (1) Overall, the normal spectral emissivity of Steel 304 specimens increased as the wavelength increased from 1.4 to 2.1 μm over a temperature range of 800 to 1100 K. (2) The fitting quality of the four-parameter LWE model was slightly superior to that of the four-parameter LLW model even though both models gave excellent fitting results. (3) The fitting quality of the LLW and LWE models essentially did not vary with heating

Table 5 Fitting results of the four-parameter LLW and LWE models at 1100 K and 30, 120, 210, and 300 min from the start of heating

T_0/K	t/min	a_0	a_1	a_2	a_3	E_{RMSE}	R
LWE	30	7.6995	-12.5525	7.3809	-1.4199	0.0098	0.9400
	120	7.7114	-12.6087	7.4913	-1.4568	0.0106	0.9233
	210	7.8109	-12.8601	7.6984	-1.5056	0.0113	0.9375
	300	8.3559	-13.8646	8.3086	-1.6242	0.0121	0.9497
LLW	30	9.1556	-17.0734	10.0463	-1.9338	0.0099	0.9383
	120	8.5219	-15.9746	9.5005	-1.8490	0.0107	0.9216
	210	8.1973	-15.4842	9.2868	-1.8188	0.0115	0.9356
	300	8.5251	-16.1085	9.6794	-1.8961	0.0124	0.9473

time. This proved that the effect of surface oxidization on the emissivity models of Steel 304 could be dismissed. In other words, the oxidization on the surface of specimens had little effect on the accurate temperature prediction based on the four-parameter LLW and LWE models.

3.2 Application of the Emissivity Models in Multispectral Radiation Thermometry

Using the least-squares technique given by Eq. (5) and the emissivity models obtained above, we could infer the surface temperature of the specimens by thermometry. By measuring the variation in the surface temperature of specimens with respect to heating time at a certain temperature, we could accurately validate whether the oxidization on the surface of specimens had an effect on the accurate prediction of the temperature, based on the emissivity models used.

In the experiments, the four-parameter LLW and LWE models were validated at temperatures from 800 K to 1100 K in increments of 20 K. During the experiments, the Steel 304 specimens were heated for 6 h at a certain temperature. When the temperatures measured by the thermocouples were compared to those inferred by thermometry, we found that the largest difference between them was basically within 20 K during the 6 h heating period. This showed that the four-parameter LLW and LWE models were suitable to predict the temperature of Steel 304. In addition, we found that the four-parameter LWE model was slightly more accurate than the four-parameter LLW model in predicting the temperature of specimens in this study.

4 Conclusions

In the present work, we studied the normal spectral emissivity characteristics of Steel 304 over a temperature range of 800 K to 1100 K and a wavelength range of 1.4 to

2.1 μm . The specimens were heated for 6 h so that the oxide layer on the surface could fully develop. The effect of surface oxidization on the emissivity models was evaluated in detail. Some important findings are summarized as follows.

(1) In general, the normal spectral emissivity of Steel 304 specimens increased with increasing wavelength from 1.4 to 2.1 μm over a temperature range of 800 to 1100 K.

(2) Both the LLW and LWE models were suitable to determine the relationship between the normal spectral emissivity and wavelength. The temperature prediction became more accurate as the number of parameters increased. In other words, the four-parameter LLW and LWE models performed the best among all the models evaluated in the present study.

(3) The four-parameter LWE model was somewhat more accurate than the four-parameter LLW model in temperature prediction over the present wavelength and temperature ranges.

(4) The effect of surface oxidization on the accurate temperature prediction of Steel 304 could be neglected when we used the four-parameter LLW and LWE models.

Acknowledgments This work is sponsored by the National Natural Science Foundation of China under Grant Nos. 61077073 and 61177092, the Program for Science and Technology Innovation Talents in Universities of Henan Province in China under Grant No. 2008HASTIT008, and the Key Program for Science and Technology Foundation of Henan Province in China under Grant No. 102102210072.

References

1. Iuchi T, *Temperature: Its Measurement and Control in Science and Technology*, (AIP Conf. Proc. 684), (ed) Ripple D C (AIP, Melville, NY) 7 (2003), p 717.
2. Furukawa T, and Iuchi T, *Rev Sci Instrum* **71** (2000) 2843.
3. Campo L D, Pérez-Sáez R B, Esquisabel X, Fernández I, and Tello M J, *Rev Sci Instrum* **77** (2006) 113111.
4. Cagran C P, Hanssen L M, Noorma M, Gura A V, and Mekhontsev S N, *Int J Thermophys* **28** (2007) 581.

5. Kobayashi M, Otsuki M, Sakate H, Sakuma F, and Ono A, *Int J Thermophys* **20** (1999) 289.
6. Shi D H, Zou F H, Wang S, Zhu Z L, and Sun J F, *IR Phys Technol* **71** (2015) 370.
7. Pujana J, del Campo L, Pérez-Sáez R B, Tello M J, Gallego I, and Arrazola P J, *Meas Sci Technol* **18** (2007) 3409.
8. Wen C-D, and Lu C-T, *J Thermophys Heat Transfer* **24** (2010) 662.
9. Wen C-D, *Int J Heat Mass Transfer* **53** (2010) 2035.
10. Wen C -D, *J Mater Eng Perform* **20** (2011) 289.
11. Shi D H, Zou F H, Wang S, Zhu Z L, and Sun J F, *IR Phys Technol* **66** (2014) 6.
12. Shi D H, Zou F H, Wang S, Zhu Z L, and Sun J F, *IR Phys Technol* **67** (2014) 42.
13. Shi D H, Zou F H, Zhu Z L, and Sun J F, *ISIJ International* **55** (2015) 697.
14. Shi D H, Pan Y W, Zhu Z L, and Sun J F, *Int J Thermophys* **34** (2013) 1100.
15. Wen C. -D and Mudawar I., *J Heat Mass Transf* **47** (2004) 3591.